Yao et al. Chin. J. Mech. Eng. (2019) 32:32
https://doi.org/10.1186/s10033-019-0344-8

Chinese Journal of Mechanical Engineering

ORIGINAL ARTICLE

Open Access

Force Analysis and Curve Design for Laying Pipe in Loop Laying Head of Wire Rod Mills

Shuangji Yao[1*], Marco Ceccarelli[2], Giuseppe Carbone[2] and Bin Ma[3]

Abstract

Laying head is a high-precision engineering device in hot-rolled high speed wire rod production line. Previously research works are focused on the laying pipe wear-resisting. Laying pipe curve design method based on wire rod kinematics and dynamics analyses are not reported before. In order to design and manufacture the laying pipe, the motion and force process of the wire rod in the laying pipe should be studied. In this paper, a novel approach is proposed to investigate the force modeling for hot-rolled wire rod in laying pipe. An idea of limited element method is used to analysis and calculates the forces between laying pipe inner surface and wire rod. The design requirements of laying pipe curve for manufacturing are discussed. The kinematics and dynamics modeling for numerical calculation are built. A laying pipe curve equation is proposed by discussing design boundary conditions. Numerical results with different laying pipe curves design parameters are plotted and compared. The proposed approach performs good result which can be applied for laying pipe curve design and analysis for engineering application.

Keywords: Wire rod mills, Laying head, Laying pipe curve design, Wire rod force analysis

1 Introduction

Manufacturing of wire rod is obtained by a high speed hot-rolled wire rod production line. As a schematic layout of the process flow shown in Figure 1 [1], a high speed hot-rolled wire rod production line contains reheating furnace, a series of rough mills, intermediate mills, finishing mills, several shears, loopers and water boxes. The finishing milled wire rod passes through several water boxes with 35–45 m length. Then the hot wire rod is quenched and controlled reduction of temperature to 750–900 °C. After the finishing rolling and water box, there is a pinch roll and laying head. With the help of a high speed rotated pipe, the laying head will change hot wire rods into convoluted form and laying the wire rod coils on the Stelmor conveyor. The coils on Stelmor conveyor will be conveyed to the next process. At the same time, Stelmor conveyor provides cooling air and the coils will be cooled and achieve the desired final properties on the Stelmor conveyor.

*Correspondence: buaayaoshuangji@163.com
[1] College of Material Science and Engineering, Yanshan University, Qinhuangdao 066004, China
Full list of author information is available at the end of the article

Laying head is one of a key and precision device in high speed production line of hot-rolled wires. Laying head device is located in water cooling section after the finishing rolling mill. The finishing mill is designed for a speed of 90–120 m/s for wire rod having a minimum diameter. Normally the mill produces series for steel wire rods diameter is between ϕ4.5 and ϕ16.0 mm [2, 3]. Thus, the speed of linear wire rods pass through the laying head is very fast while the laying head is rotating. The hot wire rods are formed into loops out of the laying head and continuously laid on a Stelmor conveyor to send to the next processes [4, 5].

Figure 2 shows the procedure of hot wire rods laying out and carrying on the Stelmor conveyor in the form of coils for air cooling. The finished hot-rolled wire rods pass through the rotated laying pipe to form coils as shown in Figure 2(a). The coils lay down onto the Stelmor conveyor and be sent to the next process is shown in Figure 2(b). In the Stelmor conveyor, cold air is blown from the bottom of the conveyor and the coils temperature is reduced, thus the color of the coils become dark before conveying to next process as shown in Figure 2(c).

The device of laying head is composed by several parts as shown in Figure 3 [1]. The input shaft (1)

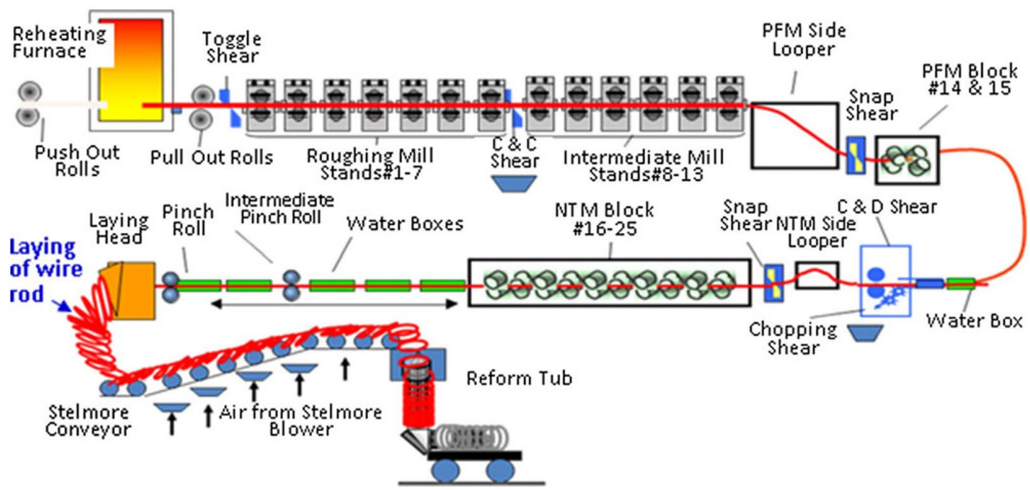

Figure 1 Schematic layout of process flow in a wire rod mill

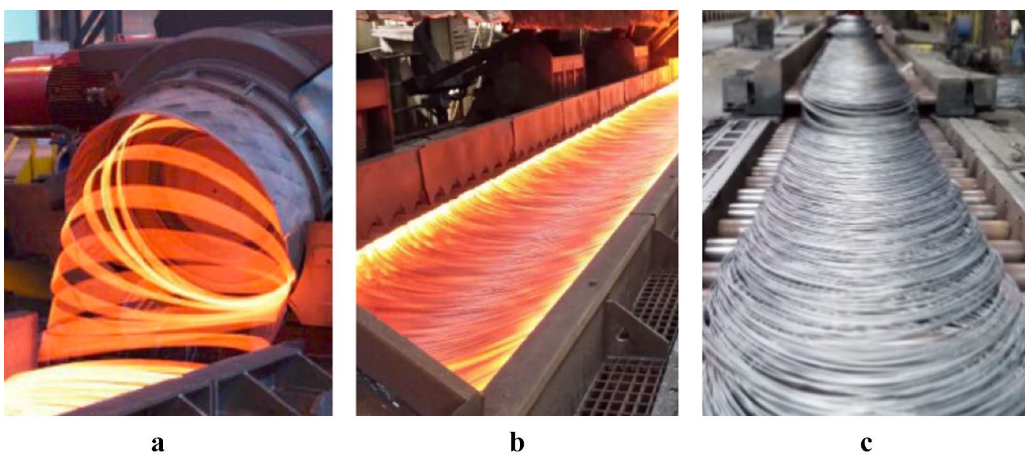

Figure 2 Laying out coils wire rod on the air cool convey: **a** coils wire out of the laying head machine; **b** hot coils wire on the air cool convey; **c** cold coils wire on the air cool convey (permission by Henan Jiyuan Iron & Steel Co., Ltd)

transmits rotation from motor. A guide pipe (3) is located at entrance of laying head device to guide the wire rod into the laying pipe (7). A pair of bevel gears (2 and 4) is assembled on the input shaft and output shaft (5). The output shaft (5) is connected with laying pipe holder (6). There are two bears located at point A and B and supporting the output shaft (5), point B to C is the cantilever part of the laying pipe holder (6). In which, laying pipe (see in Figure 4) is the most important part for this laying head device. The diagram of a laying pipe can be seen in Figure 4.

Normally the linear speed of wire rod feeding into laying head is very fast. The maximum feed speed for the minimum dimension wire rod (ϕ5.5 mm) is more than 100 m/s in the rolling scheme. The laying pipe is a 3D pipe with a complicated space curve. Some laying pipes are shown in Figure 5(a) and (b).

The output shaft continually rotates, meanwhile the linear wire rod pass into the rotated laying pipe from the entry and throughout from the exit. In this process, the wire rod is formed to be looped shape as coils and fall down on the conveyer. The dimension of the formed coils is decided by the radius of the laying pipe exit [6–8].

Laying pipe is an important part in laying head device for hot rolled high speed wire rod production line. Most of the research works of laying pipe are presented by patents. Some mechanical structures for high speed laying head devices are proposed in Refs. [9–11]. The speed relationship between laying head and rolling mill is presented in Ref. [12] for control. Fiorucci tried different

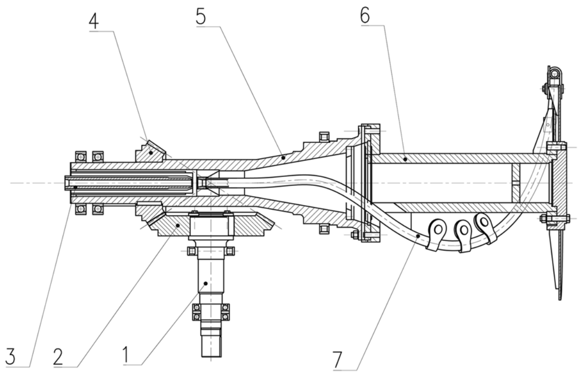

Figure 3 A design scheme of laying head machine

materials used for laying pipe in Refs. [13, 14], and some new design schemes to improve the wearing resistance property for laying pipes are reported in Refs. [15–17]. The manufacturing device and operating process for laying pipe is presented in Ref. [18]. A curve design and load analysis method is presented in Ref. [19], which is benefit for laying pipe applies theoretically. An optimal design of the Morgan Construction Companies' laying pipe is investigated in Ref. [20] to deal with uneven wear. A pipe design approach is developed to minimize and evenly distribute wear on the inner surface of laying pipe. Some researchers have provided ideas to improve the laying hand performance in modeling, design and application [9, 21–27].

Most of the mentioned research work focused on the wear-resisting for laying pipe application. The wire rod kinematics and dynamics performance while passing through the laying pipe is not referred. Therefore, the design method based on wire rod kinematics and dynamics analysis for laying pipe curve cannot be carried out. Thus, the study on the topic of wire rod force analysis in laying pipe is a research gap before.

In this paper, a method for laying pipe design, as well as the kinematics and dynamics modeling for the wire rod

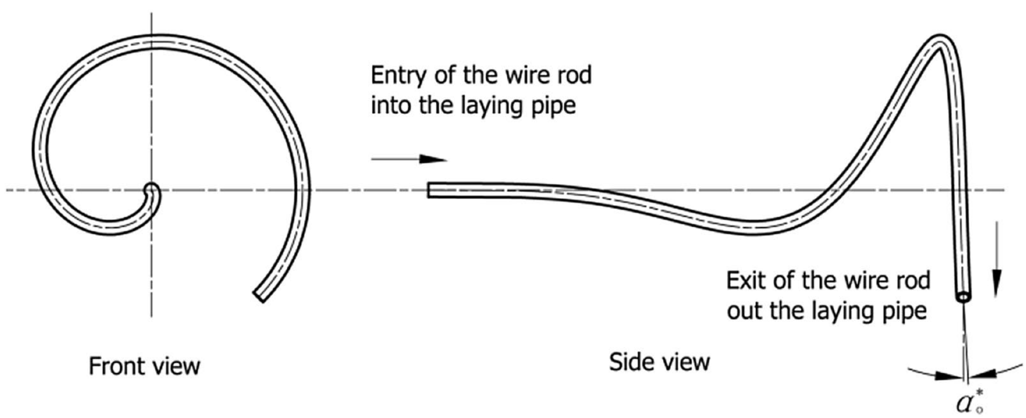

Figure 4 A diagram of a laying pipe

Figure 5 Laying head pipe before assemble: **a** laying head pipe from entrance side; **b** laying head pipe from exit side

passing in the laying pipe are proposed. The first section introduces the hot rolled high speed wire rod production line. The function and structure of the laying head machine is described. It is pointed out that the laying pipe is the key issue for the laying head. In the second section, design requirements for the laying pipe are discussed. The problems for pipe curve, laying head working stability and speed relationships are mentioned. In the third section, a method of kinematics and dynamics analysis for wire rod in the pipe is proposed to characterize the process of wire rod in the laying pipe. We also proposed a new method for laying pipe design in fourth section. The numerical computation results for the designed laying pipe are compared with existing laying pipes in the fifth section. The numerical results indicated the feasibility of the proposed design method and kinematics and dynamics modeling. It is also provided a method for laying pipe parameters choosing and discussing.

2 Design Requirements for the Laying Head Pipe

The wire rod is pinched and feed into rotated laying pipe by pinch roll as shown in Figure 1. The wire rod in the laying pipe is effect by the pipe inner surface and its shape is changed from a straight line into coils. There are friction force, centrifugal force, inertial force and supporting force impacted on wire rod [28]. The entire forces act on the wire rod together and the wire is bended according the laying pipe curve and formed into coils to achieve the desired radius at the exit as Figure 2. The requirements for the laying head pipe in a stable working condition can be explain from three aspects.

2.1 Speed Requirement

In the process of continuous rolling product line, it is necessary for laying head to match the speed relationship with pinch roll and finish mill. The linear speed of each machine should be maintained to match in a certain ratio in rolling process [29]. If the speed in one of the device is changed by the requirements of rolling production process flow, the speed of others devices should be changed relatively to maintain the matched relationship. In order to lay out coils stably and continually, the laying head will always follows the speed with pinch roll and finish mill. If the matched speed relationship cannot be kept, there would be an accident on the high speed wire rod product line. The hot-rolled wire rod will be pulled into two pieces or push toghter and be crowded out of the passing line as shown in Figure 6.

Another speed matching should also be maintained for the wire rod feed in and out the laying pipe. The feeding speed of wire rod into laying pipe is defined as v_f, the radius at the exit of the laying pipe is defined as R_0, ω_0 is the rotation speed of laying head output shaft. According the law of equal metal mass flow per second [29], there should be a balance relationship between the metal in and out the laying pipe which can be expressed as

$$v_{\mathrm{f}} = \omega_0 R_0. \tag{1}$$

If the balance of Eq. (1) is disturbed, the laying head will work unstable and the coils will be formed in different dimensions.

2.2 Laying Pipe Curve Requirement

The curve of laying pipe should be designed smoothly for the wire rod passing through easily. The requirement of the coils diameter is ensured by the exit position of the laying pipe. The speed of coils leave the laying pipe should be very small to ensure the coils can fall on the conveyer freely as shown in Figure 7.

2.3 Wear-Resisting Requirement

The laying pipe should be used for long term and cannot be worn easily. The worn is caused by the friction force on the inner surface of laying pipe. The curve should be designed smoothly to prevent the wire rod be worn sharply in some position. An ideal laying pipe curve can make the wire rod pass through comfortably. In this situation, the friction force will be decreased and will not be concentrated in small section of the laying pipe. As the result, the laying pipe will be used for a long term and the laying head working stability is improved.

3 Kinematics and Dynamics Modeling

What we desire is an arm exoskeleton which is capable of following motions of the human upper-limb accurately and supplying the human upper-limb with proper force feedback if needed. In order to achieve an ideal

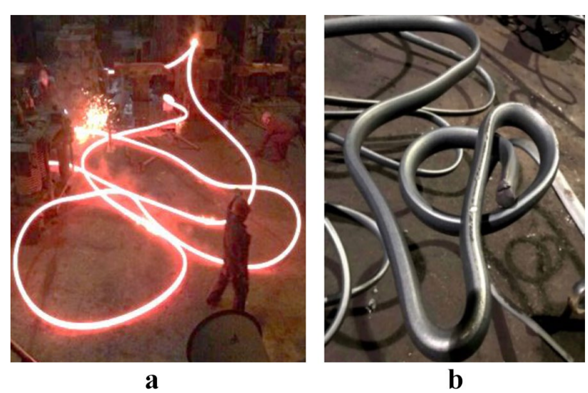

Figure 6 A producing accident: wire rod pushed toghter and crowded out of the passing line, caused by speed relationship mismatched: **a** wire rod out of the passing line; **b** the pushed toghter and crowded wire rod

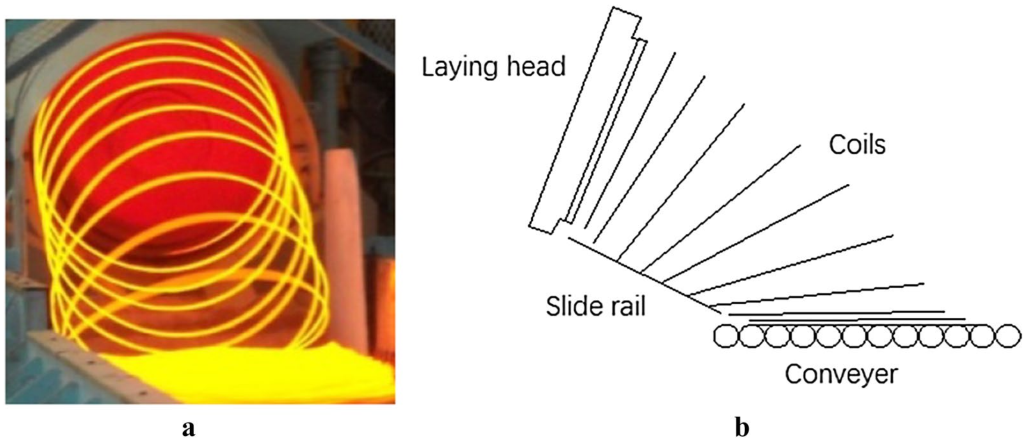

Figure 7 Appropriate coils dimension and motion at the exit of laying pipe: **a** regular coils dimension; **b** the ideal coils' motion at the exit of laying pipe

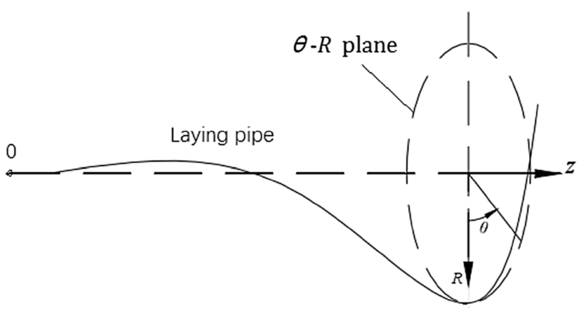

Figure 8 Cylindrical coordinates for laying pipe

controlling performance, we have to examine the structure of the human upper-limb.

3.1 Kinematics Analysis for the Wire Rod Motion in the Laying Pipe

A cylindrical coordinate is built and used to describe the curve of laying pipe as shown in Figure 8.

The origin of the cylindrical coordinates $0-R\theta Z$ is set at the entrance of laying pipe. In which, θ and R are described in a polar coordinates plane. Thus, the pipe curve $\boldsymbol{\delta}(R,\theta,Z)$ in this cylindrical coordinate can be formulated as

$$\begin{cases} R = R(t), \\ \theta = \theta(t), \quad 0 \le t \le T_0, \\ Z = Z(t), \end{cases} \tag{2}$$

where θ is the rotated angle in the plane of $\theta-R$; R is the displacement of radial direction in the plane of $\theta-R$; Z is the displacement of axial direction in the cylindrical coordinate; T_0 is the boundary condition for the variable parameter t.

The wire rod will pass through the laying pipe according the curve of Eq. (2), the velocity of the wire rod motion in the laying pipe can be deduced from the laying pipe curve. The wire rod in the pipe is selected as the object for study, the laying pipe is considered as a relative coordinate system. Thus, the velocity of a point of the wire rod in the pipe can be expressed as vector of $\vec{\boldsymbol{v}}_\mathrm{T}$,

$$\vec{\boldsymbol{v}}_\mathrm{T} = v_r\vec{\boldsymbol{e}}_r + v_\theta\vec{\boldsymbol{e}}_\theta + v_z\vec{\boldsymbol{e}}_z, \tag{3}$$

where $\vec{\boldsymbol{e}}_r$, $\vec{\boldsymbol{e}}_\theta$, $\vec{\boldsymbol{e}}_z$ represent unit direction vectors in radial direction r, tangential direction θ and axial direction z; v_r, v_θ, v_z are the velocity in each direction respectively.

Take derivative of Eq. (2) with parameter t, it can be expressed as

$$\begin{cases} v_r = R'(t), \\ v_\theta = \theta'(t)R(t), \qquad 0 \le t \le T_0. \\ v_z = Z'(t), \end{cases} \tag{4}$$

According the law of equal metal mass flow per second [29], the relative velocity between the wire rod and laying pipe is always equal to the feed speed v_f. The unit vector of the velocity vector $\vec{\boldsymbol{v}}_\mathrm{T}$ in Eq. (3) can be expressed as

$$\frac{\vec{\boldsymbol{v}}_\mathrm{T}}{|\vec{\boldsymbol{v}}_\mathrm{T}|} = \frac{v_r}{|\vec{\boldsymbol{v}}_\mathrm{T}|}\vec{\boldsymbol{e}}_r + \frac{v_\theta}{|\vec{\boldsymbol{v}}_\mathrm{T}|}\vec{\boldsymbol{e}}_\theta + \frac{v_z}{|\vec{\boldsymbol{v}}_\mathrm{T}|}\vec{\boldsymbol{e}}_z, \tag{5}$$

where $|\vec{\boldsymbol{v}}_\mathrm{T}| = (v_r^2 + v_\theta^2 + v_z^2)^{1/2}$. Thus, the relative velocity between the wire rod and laying pipe can be expressed in vector form as

$$\begin{aligned} \vec{\boldsymbol{v}}_\mathrm{g} = \frac{\vec{\boldsymbol{v}}_\mathrm{T}}{|\vec{\boldsymbol{v}}_\mathrm{T}|} \cdot v_\mathrm{f} &= \frac{v_r v_\mathrm{f}}{|\vec{\boldsymbol{v}}_\mathrm{T}|}\vec{\boldsymbol{e}}_r + \frac{v_\theta v_\mathrm{f}}{|\vec{\boldsymbol{v}}_\mathrm{T}|}\vec{\boldsymbol{e}}_\theta + \frac{v_z v_\mathrm{f}}{|\vec{\boldsymbol{v}}_\mathrm{T}|}\vec{\boldsymbol{e}}_z \\ &= (v_\mathrm{r})_\mathrm{g}\vec{\boldsymbol{e}}_r + (v_\theta)_\mathrm{g}\vec{\boldsymbol{e}}_\theta + (v_\mathrm{z})_\mathrm{g}\vec{\boldsymbol{e}}_z, \end{aligned} \tag{6}$$

where $(v_r)_g$, $(v_\theta)_g$, $(v_z)_g$ are the components of $\vec{v}_g$ in $\vec{e}_r$, $\vec{e}_\theta$, $\vec{e}_z$ directions respectively. In order to obtain the relative acceleration, take the derivative of Eq. (6) with parameter t at first. The relative acceleration of wire rod motion $\vec{a}_g$ can be expressed in form of

$$\vec{a}_g = (a_r)_g\vec{e}_r + (a_\theta)_g\vec{e}_\theta + (a_z)_g\vec{e}_z. \tag{7}$$

The relative velocities in Eq. (6) can be formulated as

$$\begin{aligned}
(v_r)'_g &= \left(\frac{v_r}{|\vec{v}_T|}v_f\right)' = \left(\frac{v'_r}{|\vec{v}_T|} - v_r\frac{v_rv'_r+v_\theta v'_\theta+v_zv'_z}{|\vec{v}_T|^2}\right)v_f,\\
(v_\theta)'_g &= \left(\frac{v_\theta}{|\vec{v}_T|}v_f\right)' = \left(\frac{v'_\theta}{|\vec{v}_T|} - v_r\frac{v_rv'_r+v_\theta v'_\theta+v_zv'_z}{|\vec{v}_T|^2}\right)v_f,\\
(v_z)'_g &= \left(\frac{v_z}{|\vec{v}_T|}v_f\right)' = \left(\frac{v'_z}{|\vec{v}_T|} - v_r\frac{v_rv'_r+v_\theta v'_\theta+v_zv'_z}{|\vec{v}_T|^2}\right)v_f.
\end{aligned} \tag{8}$$

It should be noticed that the motion of the wire rod in tangential direction $\vec{e}_\theta$ is circular motion. Thus, there should be a centripetal acceleration in the radial direction of $\vec{e}_r$, which can be formulated

$$(a_c)_g = \frac{(v_\theta)^2_g}{R} = \left(\frac{v_\theta v_f}{|\vec{v}_T|}\right)^2/R. \tag{9}$$

Thus, the relative acceleration for each direction in Eq. (7) can be expressed as

$$\begin{aligned}
(a_r)_g &= (v_r)'_g - (a_c)_g\\
&= \left(\frac{v'_r}{|\vec{v}_T|} - v_r\frac{v_rv'_r+v_\theta v'_\theta+v_zv'_z}{|\vec{v}_T|^2}\right)v_f - \left(\frac{v_\theta v_f}{|\vec{v}_T|}\right)^2/R,\\
(a_\theta)_g &= (v_\theta)'_g = \left(\frac{v'_\theta}{|\vec{v}_T|} - v_r\frac{v_rv'_r+v_\theta v'_\theta+v_zv'_z}{|\vec{v}_T|^2}\right)v_f,\\
(a_z)_g &= (v_z)'_g = \left(\frac{v'_z}{|\vec{v}_T|} - v_r\frac{v_rv'_r+v_\theta v'_\theta+v_zv'_z}{|\vec{v}_T|^2}\right)v_f.
\end{aligned} \tag{10}$$

In order to obtain the final equation of Eq. (10), take derivative of Eq. (4) with parameter t, and expresses as

$$\begin{cases}
a_r = v'_r = R''(t),\\
a_\theta = v'_\theta = \theta''(t)R(t) + \theta'(t)R'(t),\\
a_z = v'_z = Z''(t).
\end{cases} \tag{11}$$

When the laying pipe curve Eq. (2) is given, the relative velocity between wire rod and laying pipe $\vec{v}_g$ can be calculated by Eq. (6) and the relative acceleration $\vec{a}_g$ can be obtained by substituting Eq. (11) into Eq. (10).

The relative motion for wire rod in laying pipe is analyzed from Eq. (2) to Eq. (11) in the moving coordinates system $0-R\theta Z$. In order to obtain the wire rod motion in the fixed coordinates system, the rotated motion of the moving coordinates $0-R\theta Z$ should be analyzed. If the laying pipe rotates at a constant speed ω_0, it means the coordinates $0-R\theta Z$ is rotating with the speed ω_0. According motion synthesis principle, the convected motion velocity $\vec{v}_e$ and acceleration $\vec{a}_e$ of the laying pipe can be expressed as

$$\begin{aligned}
\vec{v}_e &= -R\omega_0\vec{e}_\theta,\\
\vec{a}_e &= -R\omega_0^2\vec{e}_r.
\end{aligned} \tag{12}$$

Because the convected motion of the laying pipe is rotation movement, there is a Coriolis acceleration $\vec{a}_c$ in the system, which can be formulated according the definition of Coriolis acceleration as

$$\begin{aligned}
\vec{a}_c &= 2\vec{\omega}_g \times \vec{v}_g = 2\omega_0(-\vec{e}_z) \times \vec{v}_g\\
&= 2(v_\theta)_g\omega_0\vec{e}_r - 2(v_r)_g\omega_0\vec{e}_\theta.
\end{aligned} \tag{13}$$

Thus, the absolute acceleration $\vec{a}_a$ for the wire rod in the laying pipe can be expressed as

$$\begin{aligned}
\vec{a}_a &= \vec{a}_g + \vec{a}_e + \vec{a}_c\\
&= (a_r)_a\vec{e}_r + (a_\theta)_a\vec{e}_\theta + (a_z)_a\vec{e}_z,
\end{aligned} \tag{14}$$

where

$$\begin{cases}
(a_r)_a = (a_r)_g - R\omega_0^2 + 2(v_\theta)_g\omega_0,\\
(a_\theta)_a = (a_\theta)_g - 2(v_r)_g\omega_0,\\
(a_z)_a = (a_z)_g.
\end{cases} \tag{15}$$

Equation (15) express the absolute acceleration components in the three directions of the cylindrical coordinate in Figure 8. The parameters of $(a_r)_a$, $(a_\theta)_a$, $(a_z)_a$ are the target of the kinematics calculation.

3.2 Dynamics Analysis for the Wire Rod Motion in the Laying Pipe

A force state of the wire rod is modeling and analyzed in this part. In order to analysis and calculate the force affection of the wire rod, the entire wire rod in the laying pipe is divided into limited sectional parts. Each part unit can be seen as an independent object with several kinds of forces acted on it. Thus, a limited elements method is proposed and applied to build the dynamics modeling of sectional wire rod unit.

The wire rod passing through the laying pipe can be seen composed by limited sectional rod units, each rod unit is assumed as a straight rod. Each of the straight rod has its unique position in the laying pipe and the divided sectional rod units are connected by its axial force in the connected surface. All the sectional units are pulled or pushed by the axial force and pass through the laying pipe. A force modeling of two units of wire rods is shown in Figure 9. If the divided sectional units are small enough, the results of this model is reasonable and available for the practical force situation.

As shown in Figure 9, the small section unit A–B, which defined as section number N, is selected to build the force modeling.

In Figure 9, $\vec{\boldsymbol{f}}_{mi}$ is the friction force on the sectional rod unit N, acted by inner surface of laying pipe; $\vec{\boldsymbol{P}}_{ni}$ is the supporting force on the section rod unit N, acted by inner surface of laying pipe; $\vec{\boldsymbol{N}}_i$ is the axial push force on the section rod unit N, acted by the section rod unit $(N-1)$; $\vec{\boldsymbol{N}}_{i+1}$ is the pull force on the section rod unit N, acted by the section rod unit $(N+1)$; $\vec{\boldsymbol{f}}_i$ is the inertia force on the section rod unit N.

The inertia force $\vec{\boldsymbol{f}}_i$ in Figure 9 can be expressed as

$$\vec{\boldsymbol{f}}_i = -m_i\vec{\boldsymbol{a}}_{ai} = -f_{ri}\vec{\boldsymbol{e}}_r - f_{\theta i}\vec{\boldsymbol{e}}_\theta - f_{zi}\vec{\boldsymbol{e}}_z, \tag{16}$$

$$\begin{cases} f_{ri} = m_i(a_r)_{ai}, \\ f_{\theta i} = m_i(a_\theta)_{ai}, \\ f_{zi} = m_i(a_z)_{ai}. \end{cases} \tag{17}$$

In Eqs. (16) and (17), m_i is the mass of the section rod unit N $(A-B)$; f_{ri}, $f_{\theta i}$ and f_{zi} are the component forces in each direction; $(a_r)_{ai}$, $(a_\theta)_{ai}$ and $(a_z)_{ai}$ are the acceleration in each directions, also mentioned in Eq. (15).

According D'Alembert's principle the dynamic equilibrium equation of the section rod unit N can be expressed as

$$\sum \vec{\boldsymbol{F}} + m_i\vec{\boldsymbol{a}}_{ai} = 0, \tag{18}$$

where $\sum \vec{\boldsymbol{F}}$ means the resultant force on the rod unit N. Eq. (18) can be divided into two directions, which are tangential force and normal force respectively. The equilibrium equations can be expressed as

$$\begin{cases} (\vec{\boldsymbol{f}}_i)_t + \vec{\boldsymbol{N}}_i + \vec{\boldsymbol{f}}_{mi} + (\vec{\boldsymbol{N}}_{i+1})_t = 0, \\ (\vec{\boldsymbol{f}}_i)_n + \vec{\boldsymbol{P}}_{ni} + (\vec{\boldsymbol{N}}_{i+1})_n = 0, \end{cases} \tag{19}$$

where $(\vec{\boldsymbol{f}}_i)_t$ is the tangential component of the inertia force on the section rod unit N; $(\vec{\boldsymbol{f}}_i)_n$ is the normal component of the inertia force on the section rod unit N; $(\vec{\boldsymbol{N}}_{i+1})_t$ is the tangential component of the pull force on the section rod unit N; $(\vec{\boldsymbol{N}}_{i+1})_n$ is the normal component of the pull force on the section rod unit N.

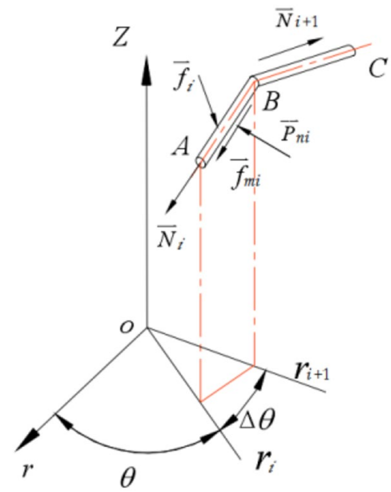

Figure 9 Force modeling of sectional divided wire rod unit

In Eq. (19), the direction of the supporting force $\vec{\boldsymbol{P}}_{ni}$ is the same as the normal of vector of section rod unit N (vector $\overrightarrow{\boldsymbol{AB}}$), the direction of the friction force $\vec{\boldsymbol{f}}_{mi}$ is the same as the tangential of vector $\overrightarrow{\boldsymbol{AB}}$.

The tangential and normal components of inertia force $\vec{\boldsymbol{f}}_i$ can be solved by using the directional cosine of the straight sectional unit N (vector $\overrightarrow{\boldsymbol{AB}}$). The unit vector in direction of vector $\overrightarrow{\boldsymbol{AB}}$ can be expressed as

$$(\overrightarrow{\boldsymbol{AB}})_i = \cos\alpha\vec{\boldsymbol{e}}_r + \cos\beta\vec{\boldsymbol{e}}_\theta + \cos\gamma\vec{\boldsymbol{e}}_z, \tag{20}$$

where $\cos\alpha$, $\cos\beta$ and $\cos\gamma$ are the directional cosine of $\vec{\boldsymbol{e}}_r$, $\vec{\boldsymbol{e}}_\theta$, $\vec{\boldsymbol{e}}_z$ in the cylindrical coordinates $0-R\theta Z$. If the position of the sectional unit A–B is known as vector $\overrightarrow{\boldsymbol{AB}}$, the direction cosine $\cos\alpha$, $\cos\beta$ and $\cos\gamma$ can be calculated.

The tangential component of the inertia force $(\vec{\boldsymbol{f}}_i)_t$ can be equated as $(f_i)_t$

$$(f_i)_t = \vec{\boldsymbol{f}}_i \cdot (\overrightarrow{\boldsymbol{AB}})_i, \tag{21}$$

$(f_i)_t$ in Eq. (21) can be expressed in cylindrical coordinate $0-R\theta Z$ as $(\vec{\boldsymbol{f}}_i)_t$ by dot product with unit vector $(\overrightarrow{\boldsymbol{AB}})_i$,

$$(\vec{\boldsymbol{f}}_i)_t = (\vec{\boldsymbol{f}}_i \cdot (\overrightarrow{\boldsymbol{AB}})_i) \cdot (\overrightarrow{\boldsymbol{AB}})_i, \tag{22}$$

thus, the normal component of the inertia force $(\vec{\boldsymbol{f}}_i)_n$ can be formulated as

$$\begin{aligned} (\vec{\boldsymbol{f}}_i)_n &= \vec{\boldsymbol{f}}_i - (\vec{\boldsymbol{f}}_i)_t \\ &= (f_{ri} - f_{ri}\cos^2\alpha - f_{\theta i}\cos\beta\cos\alpha - f_{zi}\cos\gamma\cos\alpha)\vec{\boldsymbol{e}}_r + \\ &= (f_{\theta i} - f_{ri}\cos\alpha\cos\beta - f_{\theta i}\cos^2\beta - f_{zi}\cos\gamma\cos\beta)\vec{\boldsymbol{e}}_\theta + \\ &= (f_{zi} - f_{ri}\cos\alpha\cos\gamma - f_{\theta i}\cos\beta\cos\gamma - f_{zi}\cos^2\gamma)\vec{\boldsymbol{e}}_z. \end{aligned} \tag{23}$$

The pull force $\vec{N}_{i+1}$ on the section rod unit N can be expressed as

$$\vec{N}_{i+1}=\vec{N}_{r(i+1)}\vec{e}_r+\vec{N}_{\theta(i+1)}\vec{e}_\theta+\vec{N}_{z(i+1)}\vec{e}_z. \tag{24}$$

The tangential vector of the pull force $\vec{N}_{i+1}$ on unite A–B can be equated as $(\vec{N}_{i+1})_t$

$$\begin{aligned}(\vec{N}_{i+1})_t&=(\vec{N}_{i+1}\cdot(\overrightarrow{AB})_i)\cdot(\overrightarrow{AB})_i\\&=(\vec{N}_{r(i+1)}\cos\alpha+\vec{N}_{\theta(i+1)}\cos\beta\\&\quad+\vec{N}_{z(i+1)}\cos\gamma)\cdot(\overrightarrow{AB})_i.\end{aligned} \tag{25}$$

Thus, the normal component of the pull force $\vec{N}_{i+1}$ can be formulated as

$$\begin{aligned}(\vec{N}_{i+1})_n&=\vec{N}_{i+1}-(\vec{N}_{i+1})_t\\&=(N_{r(i+1)}-N_{r(i+1)}\cos^2\alpha-N_{r(i+1)}\cos\beta\cos\alpha-N_{r(i+1)}\cos\gamma\cos\alpha)\vec{e}_r+\\&=(N_{r(i+1)}-N_{r(i+1)}\cos\alpha\cos\beta-N_{r(i+1)}\cos^2\beta-N_{r(i+1)}\cos\gamma\cos\beta)\vec{e}_\theta+\\&=(N_{r(i+1)}-N_{r(i+1)}\cos\alpha\cos\gamma-N_{r(i+1)}\cos\beta\cos\gamma-N_{r(i+1)}\cos^2\gamma)\vec{e}_z.\end{aligned} \tag{26}$$

According Eq. (19), the contact force of the sectional rod unit N can be formulated from the normal force equilibrium equation as

$$\vec{P}_{ni}=-(\vec{f}_i)_n-(\vec{N}_{i+1})_n=P_{ri}\vec{e}_r+P_{ri}\vec{e}_\theta+P_{ri}\vec{e}_z. \tag{27}$$

The friction force $\vec{f}_{mi}$ between rod unit N and inner surface of laying pipe can be formulated by Coulomb's law of friction as

$$\vec{f}_{mi}=-\mu\left|\vec{P}_{ni}\right|\cdot(\overrightarrow{AB})_i. \tag{28}$$

According Eq. (19), the axial push force $\vec{N}_i$ on the section rod unit N can be formulated from the tangential force equilibrium equation as

$$\vec{N}_i=-(\vec{f}_i)_t-\vec{f}_{mi}-(\vec{N}_{i+1})_t. \tag{29}$$

Thus, Eq. (19) can be solved if N_{i+1} is given as a known parameters from laying pipe working boundary condition.

3.3 Boundary Conditions

It can be concluded that the inertia force $\vec{f}_i$ can be calculated by providing the equation of laying pipe curve and the rotation speed of the laying head. Thus, the contact force $\vec{P}_{ni}$, friction force $\vec{f}_{mi}$ and push or pull force $\vec{N}_i$ for the sectional unite in the laying pipe can be calculated by Eqs. (27), (28) and (29), if the vector force $\vec{N}_{i+1}$ is known as an initial parameter.

For the proposed dynamics modeling of the wire rod in the laying pipe, boundary conditions are necessary to solve the force equilibrium Eq. (19). Boundary conditions for this modeling can be found at the entry and exit of the laying pipe as shown in Figure 10.

3.3.1 Boundary Conditions at the Entrance of the Laying Pipe

There is a speed relationship between the wire rod feeding speed v_f and the rotated speed of laying pipe ω_0 at the

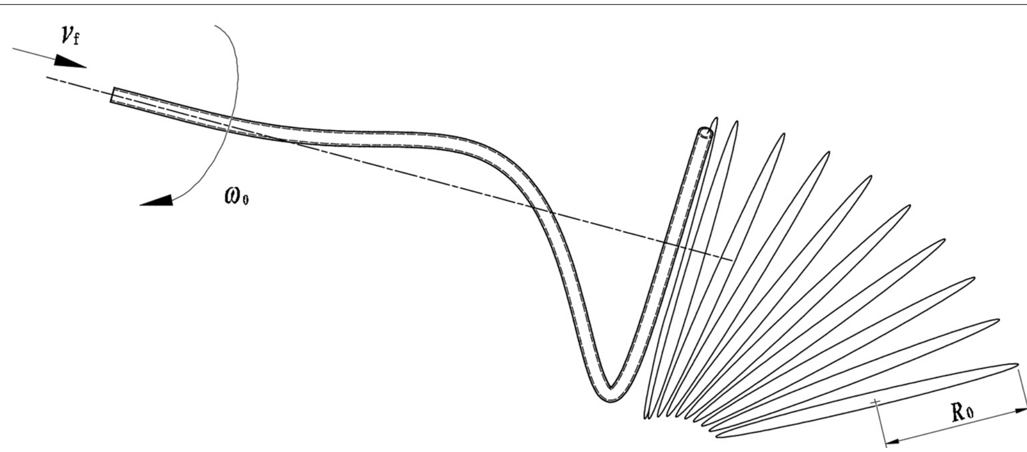

Figure 10 Working condition of the laying pipe

entry of the laying pipe, which has been formulated as $v_f = \omega_0 R_0$ in Eq. (1) of Section 2. The wire rod at the entry of the laying pipe should keep the relationship in Eq. (1) and it can be a boundary conditions at the entrance of the laying pipe.

3.3.2 Boundary Conditions at the Exit of the Laying Pipe

As shown in Figure 10, the wire rod sectional unit at the laying pipe exit will not push or pull its adjacent units along their centerline of the wire rod. There is only gravity force impacted on the wire coils at the pipe exit to make the coils fall on the conveyer freely and slowly. Thus, the pull force on the final section unit N of the wire rod is zero, which can be expressed as

$$\vec{\boldsymbol{N}}_{N+1} = 0. \tag{30}$$

Let's select the sectional unit at the exit of laying pipe to study, at this unique moment $\vec{\boldsymbol{N}}_{N+1}$ is a boundary condition for Eq. (19) as expressed in Eq. (30). Thus, the force balance Eq. (19) of the final unit can be solved. For rod unit N, the result of push force $\vec{\boldsymbol{N}}_N$ in Eq. (19) can be calculated and the result $\vec{\boldsymbol{N}}_N$, seen as the pull force for rod unit $N-1$, can be used as a given parameter in the rod unit $N-1$ force balance equation. Thus, all the forces on each sectional unit can be calculated by providing computed result $\vec{\boldsymbol{N}}_i$ as a given parameter for $i-1$ unit. Thus, the sectional units force equilibrium equations (19) will be solved one by one from the final sectional unit to the first sectional unit.

3.4 Numerical Procedure for the Wire Rod Dynamics Analysis

A numerical calculation procedure for the proposed modeling can be carried out based on the above-mentioned kinematics and dynamics analysis to compute the velocity and forces of the wire rod in the laying pipe.

In order to solve the velocity and forces of the wire rod, some parameters should be given as the initial conditions for the numerical procedure calculation. The curve equation $\boldsymbol{\delta}(R, \theta, Z)$, the feed speed of the linear wire rod v_f and the rotation speed of the laying pipe ω_0 should also be given as the parameters for the kinematics and dynamics modeling.

It is assumed that the wire rod in the laying pipe always moves along the center of the laying pipe. Thus, the laying pipe curve equation can be used to describe the wire rod path in the laying pipe. The numerical procedure for the wire rod kinematics and dynamics calculation flowchart is shown in Figure 11. In this

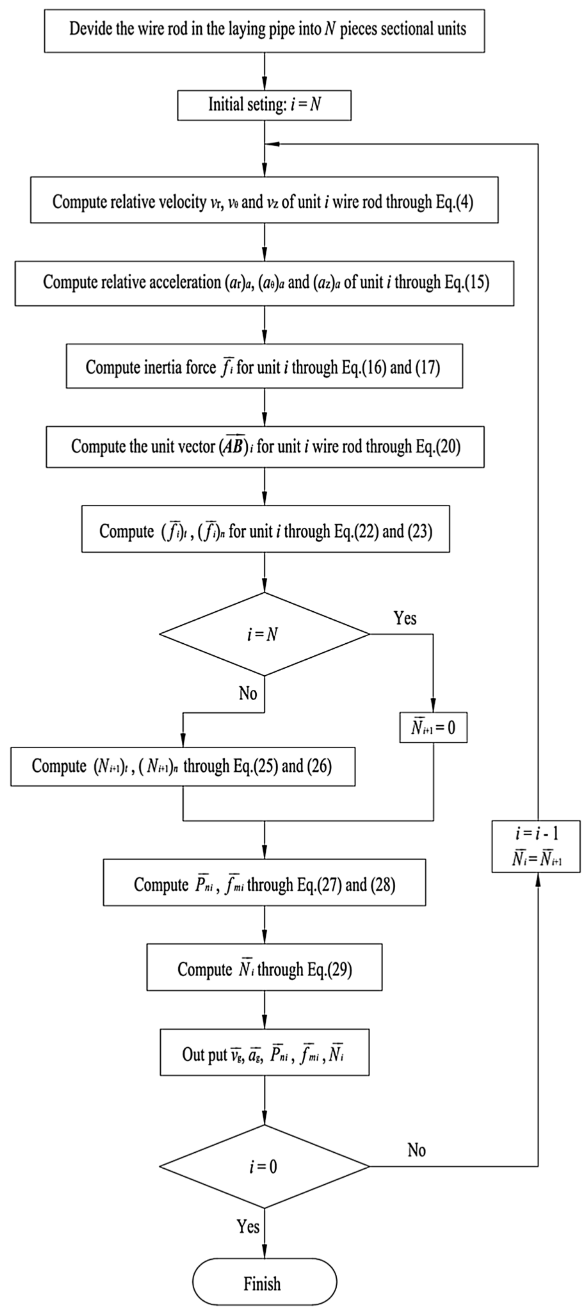

Figure 11 Numerical procedure for the kinematics and dynamics analysis

flowchart, the laying pipe curve equation $\boldsymbol{\delta}(R, \theta, Z)$, the feed speed of the linear wire rod v_f before laying head and the rotation speed of the laying pipe ω_0 are given as initial conditions. Another boundary condition is the pull force $\vec{\boldsymbol{N}}_{i+1}$ of the final sectional unit (unit N) which is equal to zero at the exit (mentioned in Eq. (30)). The flowchart of this numerical procedure can output the relative velocity $\vec{v}_g$ and acceleration $\vec{a}_g$ of the wire rod in laying pipe as well as the connect force $\overrightarrow{P}_{ni}$, the friction force $\vec{f}_{mi}$ and the axial force for push or pull in the wire rod centerline.

4 Boundary Conditions Discussion and Laying Pipe Curve Design

4.1 Boundary Conditions for the Laying Pipe Curve Design

The curve of the laying pipe $\boldsymbol{\delta}(R,\theta,Z)$ are described in cylindrical coordinate $0-R\theta Z$ shown in Figure 8. The pipe curve in this cylindrical coordinate can be formulated as Eq. (2), and Eq. (2) can also been seen as the description equation for wire rod motion path in the laying pipe:

$$\begin{cases} R = R(t), \\ \theta = \theta(t), \\ Z = Z(t), \end{cases} \qquad 0 \le t \le T_0.$$

Some known conditions can be concluded at the laying pipe entry and exit:

When the wire rod passing through the entry ($t=0$), the position components in R, θ and Z directions are all zero; the velocities components in R, θ and Z directions are 0, v_f and 0 respectively.

When the wire rod passing through the exit ($t=T_0$), the position components in R, θ and Z directions are R_0, θ_0 and Z_0; The velocities components in R, θ and Z are 0, 0 and ω_0 respectively.

According to the above boundary conditions, the laying pipe curve can be given as:

$$t = 0, \quad \begin{cases} R(0) = 0;\ Z(0) = 0;\ \theta(0) = 0, \\ \frac{dR}{dt} = 0;\ \frac{dZ}{dt} = |v_f|;\ \frac{d\theta}{dt} = 0, \end{cases} \tag{31}$$

$$t = T_0, \quad \begin{cases} R(T_0) = R_0;\ Z(T_0) = Z_0;\ \theta(T_0) = \theta_0, \\ \frac{dR}{dt} = 0;\ \frac{dZ}{dt} = 0;\ \frac{d\theta}{dt} = \omega_0, \end{cases} \tag{32}$$

where the design parameters for the laying pipe curve are as follows: T_0 is the time for a wire rod point passing through the laying pipe; R_0 is the radius dimension of laying pipe at the exit; θ_0 is the rotation angle of laying pipe curve at the exit; Z_0 is the dimension of coordinate Z for laying pipe exit.

Actually, according our experience, when we focused on the exit of the laying pipe, dZ/dt is not exactly equal to 0. There should be a small angle at the laying pipe exit according the plane R-θ, which is defined as α_o^* and can be shown in Figure 4. The small angle α_o^* is used to ensure the wire coils out of the laying pipe easily and could fall down on the conveyor with very small velocity. Usually, the angle $\alpha_0^* \in [1.6°, 2.5°]$. Thus, the boundary conditions for the laying pipe curve design can be developed as

$$t = 0, \quad \begin{cases} R(0) = 0;\ Z(0) = 0;\ \theta(0) = 0, \\ \frac{dR}{dt} = 0;\ \frac{dZ}{dt} = v_f;\ \frac{d\theta}{dt} = 0, \end{cases} \tag{33}$$

$$t = T_0, \quad \begin{cases} R(T_0) = R_0;\ Z(T_0) = Z_0;\ \theta(T_0) = \theta_0, \\ \frac{dR}{dt} = 0;\ \frac{dZ}{dt} = v_f \sin\alpha_0^*;\ \frac{d\theta}{dt} = \omega_0. \end{cases} \tag{34}$$

The boundary conditions in Eqs. (33) and (34) should satisfy the proposed laying pipe curve equation. These known conditions will help us to choose the form and parameters for laying pipe curve equation.

4.2 Curve Equation Design for the Laying Pipe Curve

In order to design the laying pipe curve equation, the parameters equations $\theta(t)$, $R(t)$, $Z(t)$ with variable t should be considered independently.

4.2.1 Relationship between Rotation Angle θ and Time t

According to the boundary conditions in Eqs. (33) and (34), the equation of rotation angle $\theta(t)$ can be formulated when $t=0$ and $t=T_0$ as

$$\begin{cases} \theta(t)|_{t=0} = 0, \\ \theta(t)\big|_{t=T_0} = \theta_0, \end{cases} \quad \begin{cases} \theta'(t)|_{t=0} = 0, \\ \theta'(t)\big|_{t=T_0} = \omega_0. \end{cases} \tag{35}$$

According Eq. (1), the laying pipe is rotated in a constant speed ω_0. Thus, the rotation angle θ and time variable t should obey a linear relationship which is

$$\theta(t) = \omega_0 t. \tag{36}$$

4.2.2 Relationship between Radial Displacement R and Time t

According boundary conditions in Eqs. (33) and (34), the equation of radial displacement R can be formulated when $t=0$ and $t=T_0$ as

$$\begin{cases} R(t)|_{t=0} = 0, \\ R(t)\big|_{t=T_0} = R_0, \end{cases} \quad \begin{cases} R'(t)|_{t=0} = 0, \\ R'(t)\big|_{t=T_0} = 0. \end{cases} \tag{37}$$

4.2.3 Relationship between Axis Displacement Z and Time t

According boundary conditions in Eqs. (33) and (34), the function of axis displacement Z can be formulated when $t=0$ and $t=T_0$ as

$$\begin{cases} Z(t)|_{t=0} = 0, \\ Z(t)\big|_{t=T_0} = Z_0, \end{cases} \quad \begin{cases} Z'(t)|_{t=0} = 0, \\ Z'(t)\big|_{t=T_0} = v_f \sin\alpha_0^*. \end{cases} \tag{38}$$

In order to highlight the characters of the functions $\theta(t)$, $R(t)$ and $Z(t)$. Functions curves are expressed according to the boundary conditions in Eqs. (35)–(38) and shown in Figure 12.

It can be seen that from the functions characters in Figure 12(a). The $\theta(t)$ is a the linear function, the function

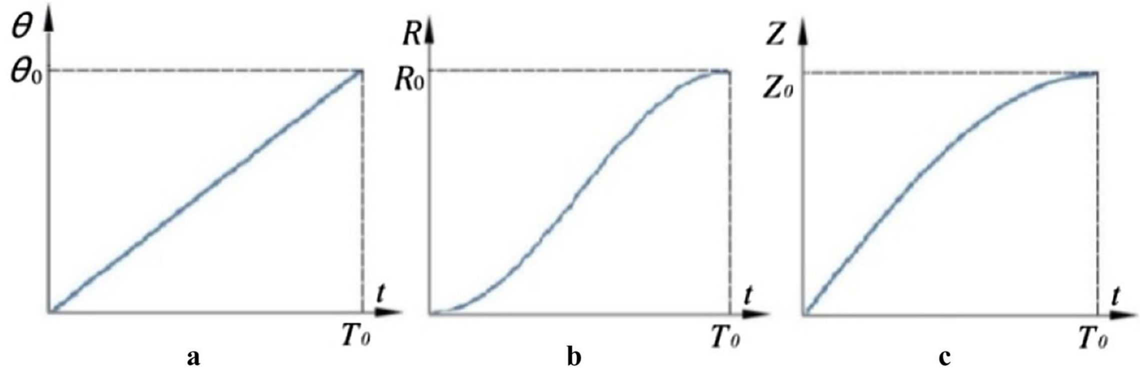

Figure 12 Functions curves characters: **a** $\theta(t)$, **b** $R(t)$, **c** $Z(t)$

characters for $R(t)$ and $Z(t)$ are similar as sine function or cosine function.

Thus, the laying pipe curve can be designed by selecting and testing many different functions and finally be defined as:

$$\begin{cases} R(t) = \frac{R_0}{T_0}t - \frac{R_0}{2\pi}\sin\left(\frac{2\pi}{T_0}t\right), \\ \theta(t) = \omega_0 t, \\ Z(t) = \frac{k^* v_f}{2}t + \frac{(2-k^*)v_f T_0}{2\pi}\sin\left(\frac{\pi}{T_0}t\right), \end{cases} \quad 0 \le t \le T_0. \tag{39}$$

Eq. (39) qualified the characters of the laying pipe curve both in the entry and exit. The boundary conditions for the laying pipe curve in Eq. (33) are also ensured by Eq. (39). According to Eqs. (38) and (39), if $t = T_0$, the equation for function $Z(t)$ can be expressed as

$$Z'(t)\big|_{t=T_0} = v_f \sin\alpha_0^* = (k^* - 1)v_f.$$

Because of $\alpha_0^* \in \left[1.6^\circ,\ 2.5^\circ\right]$, thus it can be concluded that

$$k^* = \sin\alpha_0^* + 1 \in [1.028,\ 1.044]. \tag{40}$$

Table 1 A solution for design parameters of laying pipe

Design parameter	Value	Design considerations
v_f (m/s)	92	Decided by rolling production process flow
R_0 (mm)	525	Decided by wire coils dimension
θ_0 (°)	350	Decided by mechanical structure of laying head
Z_0 (mm)	1623.4	Decided by mechanical structure of laying head
ω_0 (rad/s)	175.24	Computed by v_f/R_0
T_0 (s)	0.035	Computed by θ_0/ω_0
k^*	1.0349	Computed by Eq. (40) set $\alpha_0^* = 2°$

The design parameters in Eq. (39) for laying pipe curve equation are decided by rolling production process, such as formed coils diameter and laying head structure. Most of these parameters have been fixed by milling process in a specific high speed wire rod production line. One of solutions for laying pipe design parameters in a high speed wire rod production line are given and list in Table 1.

Thus, with the solution for design parameters in Table 1, the final designed laying pipe curve equation $\boldsymbol{\delta}_1(R, \theta, Z)$ can be expressed as

$$\delta_1: \begin{cases} R(t) = 15000t - 83.56\sin(179.52t), \\ \theta(t) = 175.24t, \\ Z(t) = 46383t + 481.79\sin(89.76t), \end{cases} \quad 0 \le t \le 0.035, \tag{41}$$

where the unit of $R(t)$ is mm, the unit of $\theta(t)$ is rad/s, the unit of $Z(t)$ is mm, respectively.

5 Numerical Results and Comparison for Laying Pipes

5.1 Laying Pipe Curves Obtain

In order to make comparison with other laying pipes, two laying pipes using in different types laying head device are selected. The pipe curves are obtained by reverse engineering with laser 3D scanning. The laser scanning device is shown in Figure 13(a), the obtained laying pipe modeling are shown in Figure 13(b) and (c). The laying pipe curves in Figure 13(b) and (c) is named $\boldsymbol{\delta}_2$ and $\boldsymbol{\delta}_3$.

According the obtained 3D modeling of $\boldsymbol{\delta}_2$ and $\boldsymbol{\delta}_3$, the laying pipe curve equations are carried out by curve fitting and be expressed as

$$\delta_2: \begin{cases} R(t) = R_2(t), \\ \theta(t) = 184.51t + 12 \times \sin(89.76t)^{2.716}, \\ Z(t) = 47071t + 631.2\sin(89.76t), \end{cases} \quad 0 \le t \le 0.035, \tag{42}$$

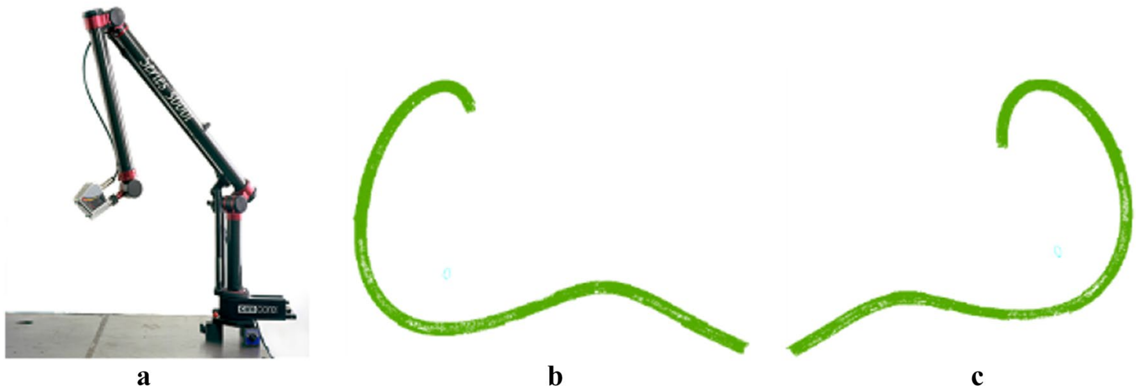

Figure 13 The reverse engineering for laying pipes: **a** laser scanning device; **b** the scanned laying pipe $\boldsymbol{\delta}_2$; **c** the scanned laying pipe $\boldsymbol{\delta}_3$

Table 2 The coordinate data for $R_2(t)$ and $R_3(t)$ function

Point in spline curve	Parameter		
	t ($\times 10^{-3}$)	R_2 (mm)	R_3 (mm)
1	0	0	0
2	3.28	67.4	16.25
3	6.9	196.6	106.2
4	10.4	301.0	248.4
5	13.9	395.7	372.9
6	17.4	443.7	452.5
7	20.9	479.1	485.1
8	24.5	505.5	494.0
9	28.0	518.7	508.3
10	31.5	523.5	520.9
11	35.0	525	525.5

$$\delta_3: \begin{cases} R(t) = R_3(t), \\ \theta(t) = -1020.1t^5 + 2842.9t^4 - 2953.4t^3 \\ \qquad +1478.3t^2 + 22.4t, \\ Z(t) = 50971t + 590.3\sin(89.76t), \end{cases} \quad 0 \le t \le 0.035. \tag{43}$$

$R_2(t)$ and $R_3(t)$ in Eqs. (42) and (43) are obtained by a series of coordinates data with t and R, which are listed in Table 2. The coordinates data are used to fit functions for $R_2(t)$ and $R_3(t)$. The of functions $R_2(t)$ and $R_3(t)$ are obtained by 10 pieces of piecewise cubic spline curve composed functions.

A modeling results with the three laying pipe curves coordinates of $\boldsymbol{\delta}_1$, $\boldsymbol{\delta}_2$ and $\boldsymbol{\delta}_3$ are shown and compared in Figure 14. Comparing with the other two laying pipe curves, the designed laying pipe curve $\boldsymbol{\delta}_1$ is much smooth between the entry and middle part of the curve.

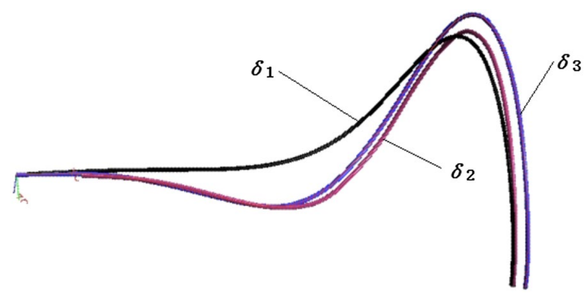

Figure 14 Comparison for three laying pipe curves as function of Eqs. (41), (42) and (43)

5.2 Numerical Computation and Comparison with Kinematics and Dynamics Results

Numerical computation are carried out for the three laying pipe curves $\boldsymbol{\delta}_1$, $\boldsymbol{\delta}_2$ and $\boldsymbol{\delta}_3$ by using the kinematics and dynamics model proposed in Section 3. The calculation procedure is following the flowchart in Figure 11. The wire rod diameter used for calculation is ϕ6.5 mm, the feed speed of wire rod is 92 m/s. Some numerical results are shown from Figure 15, 16, 17 Figure 18.

Figure 15 shows the numerical results for wire rod in laying pipes. It can be seen that the wire rod relative velocities in three laying pipes have the same tendency. The relative velocities in axial direction v_z are all equal to the feed speed v_f at the entry, and decrease meanwhile the wire rod is passing in the laying pipe. Finally it is nearly zero at the exit. The relative velocities in tangential direction are v_θ are all zero at the entry, and change to nearly feed speed v_f at the exit of the laying pipe. The relative velocities in radial direction are v_r are all zero at the entry and change to the maximum in the middle part of the laying pipe, then it is decreased to zero at the exit of laying pipe.

Comparing with $\boldsymbol{\delta}_2$ and $\boldsymbol{\delta}_3$, the maximum value of v_θ for designed laying pipe is appeared nearly the exit of

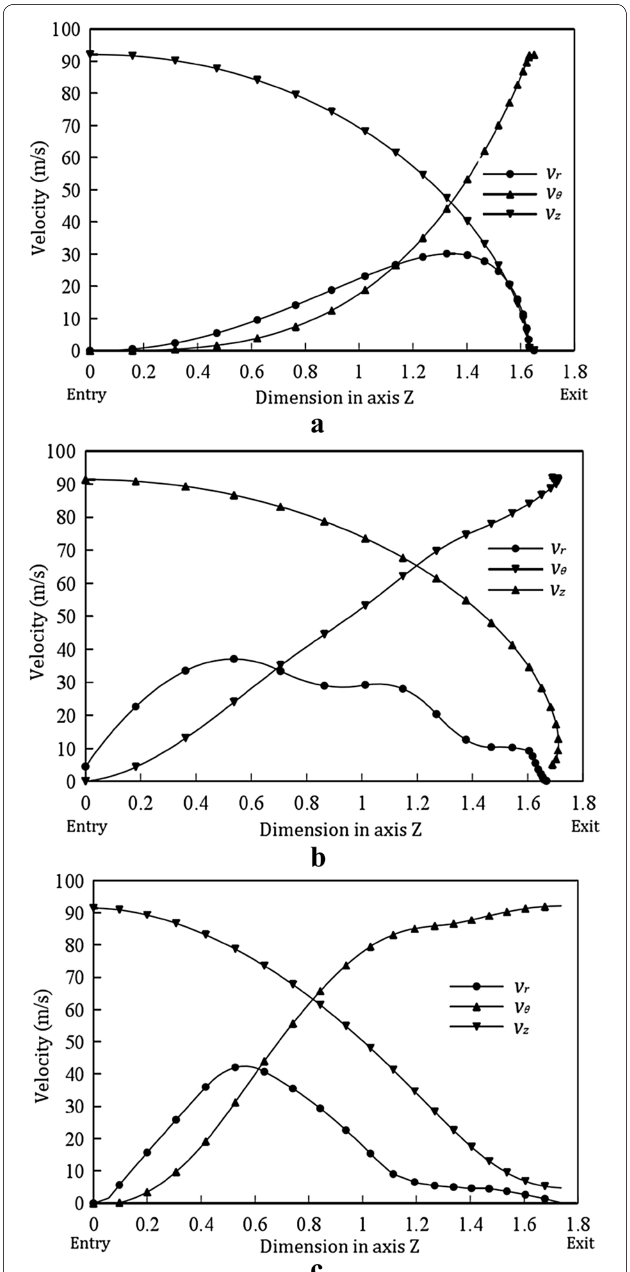

Figure 15 Numerical results for wire rod relative velocity in different laying pipes: **a** relative velocity in laying pipe curve $\boldsymbol{\delta}_1$; **b** relative velocity in laying pipe curve $\boldsymbol{\delta}_2$; **c** relative velocity in laying pipe curve $\boldsymbol{\delta}_3$

the pipe. It is caused by the smooth curve between the pipe entry and middle part, and the wear of the laying pipe inner surface will be reduced in this position. The variable characters of the wire rod relative velocity in Figure 15 ensure the laying pipes has only axial velocity at entry and has only tangential velocity at exit. The resultant velocity of the three velocities components is equal to the feed speed v_{f} at any time in Figure 15.

The dynamic numerical results for wire rod motion in laying pipes are shown from Figure 16 to Figure 18. Figure 16 indicates that the axial force for wire rod in the three laying pipes. The tendency of axial forces is 33–43 MPa at the pipe entry, and increases to the maximum after 1.0–1.2 m then the axial forces decrease to zero at the exit of laying pipe. The maximum value axial force in laying pipe $\boldsymbol{\delta}_1$ is 48 MPa; the maximum value axial forces in laying pipe $\boldsymbol{\delta}_2$ and $\boldsymbol{\delta}_3$ are 36 MPa.

Figure 17 and Figure 18 are the support forces and friction forces for the wire rod passing in the three laying pipes. According the Coulomb's law of friction, the relationship between friction force and support force are proportional. The maximum friction force in unit length is 0.78 N/mm for the designed laying pipe $\boldsymbol{\delta}_1$. It appears at 1.35 m after laying pipe entry. The position with maximum friction force will be the worn out position when the laying pipe is used. Comparing with laying pipes $\boldsymbol{\delta}_2$ and $\boldsymbol{\delta}_3$, the worn out position in $\boldsymbol{\delta}_1$ is farther away from pipe entry than others. Because the designed laying pipes curve $\boldsymbol{\delta}_1$ is much smooth in the middle part than $\boldsymbol{\delta}_2$ and $\boldsymbol{\delta}_3$ in Figure 14. Thus, the maximum friction position is changed.

5.3 Numerical Results and Comparison with Different Design Parameters

In this section, some different values of parameters are changed for the designed laying pipe curve. Numerical results are carried out to discuss the dynamic performance with different design parameters. The initial design parameters are list in Table 1, and the wire rod dimension is ϕ6.5 mm.

Figure 19 shows the wire rod axial force and friction force performance with different feed speed v_{f}. According the law of equal metal mass flow per second, the relationship between the feed speed v_{f} and rotation speed of laying head output shaft ω_0 formulated in Eq. (1) should be kept. Thus, the numerical results for v_{f} equals 70 m/s, 90 m/s and 110m/s should match the ω_0 with 1273 r/min, 1637 r/min and 2000 r/min, respectively.

It can be seen that the maximum value of axial force in Figure 19(a) are 30 MPa, 43 MPa and 72 MPa, respectively for different feed speeds. The axial force is increased obviously when the feed speed is 110 m/s. In Figure 19(b), the maximum friction force in 110 m/s is about twice as much as 90 m/s. Comparing with other feed speed, when the feed speed is 110/m, the laying pipe will be worn out first. Actually, the higher feed speed will lead to fast wearing out, it has been verified in other wire rod rolling plant.

It should be noticed that, the tensile strength limitation for most hot-rolled rod materials are less than 70 MPa in

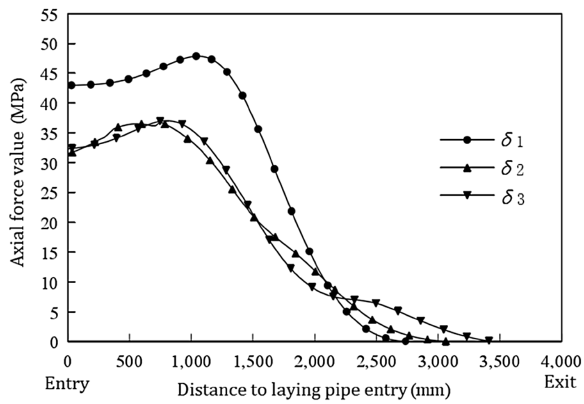

Figure 16 Axial force for three laying pipes

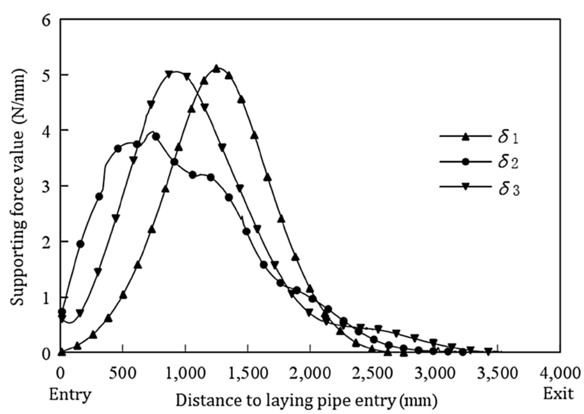

Figure 17 Supporting force for three laying pipes

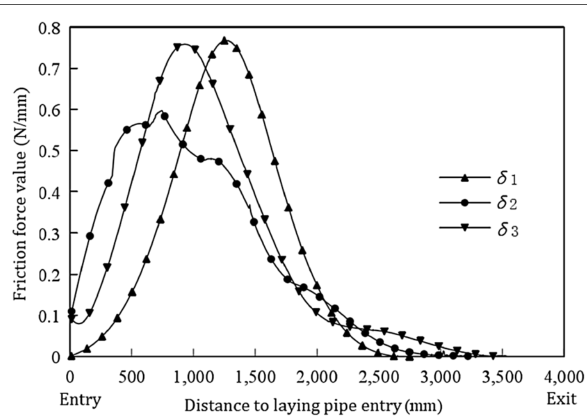

Figure 18 Friction force for three laying pipes

the temperature range of 750–900 °C. Thus, the wire rod will be pulled broken into pieces if the laying pipe curve working with $v_f = 110$ m/s. Thus, there should be a new

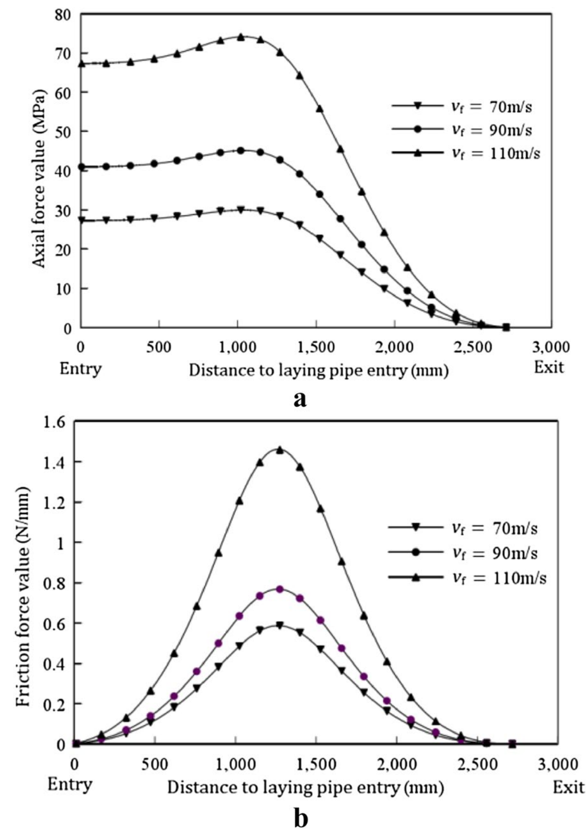

Figure 19 Numerical results with different feeding speed: **a** Axial force in the design laying pipe; **b** Friction force in the design laying pipe

designed laying pipe curve for the higher feed speed and rotation speed.

According to Figure 20(a) and (b) the axial force and friction force will be less if the axial dimension Z_0 is increasing. Thus, increasing the axial dimension Z_0 will be benefit for the wire rod force impaction in the laying pipe. On the other hand, enlarge laying pipe axial dimension Z_0 will lead the pipe holder cantilevers out too far as shown in Figure 3. Thus, the dynamic balance will be difficult for the output shaft rotating.

Figure 21 shows the wire rod axial force and friction force performance with different laying pipe curve rotated angle θ_0. It can be seen from Figure 21(a) that the axial forces will increase if the curve rotated angle θ_0 is increased. The friction force will decrease if the curve rotated angle θ_0 is increased in Figure 21(b). Thus, it can be concluded that increasing the curve rotated angle θ_0 will be benefit for reducing the friction force of the laying pipe, meanwhile the axial force should not more than the tensile strength limitation for the wire rod. The rotated angle $\theta_0 \in [350°, 400°]$ is a good choice for pipe design.

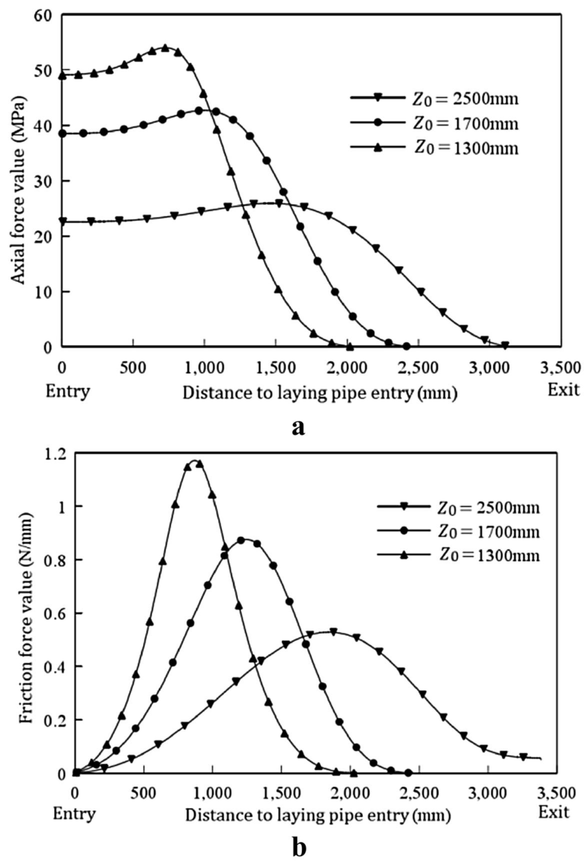

Figure 20 Numerical results with different Z_0: **a** Axial force in the design laying pipe; **b** Friction force in the design laying pipe

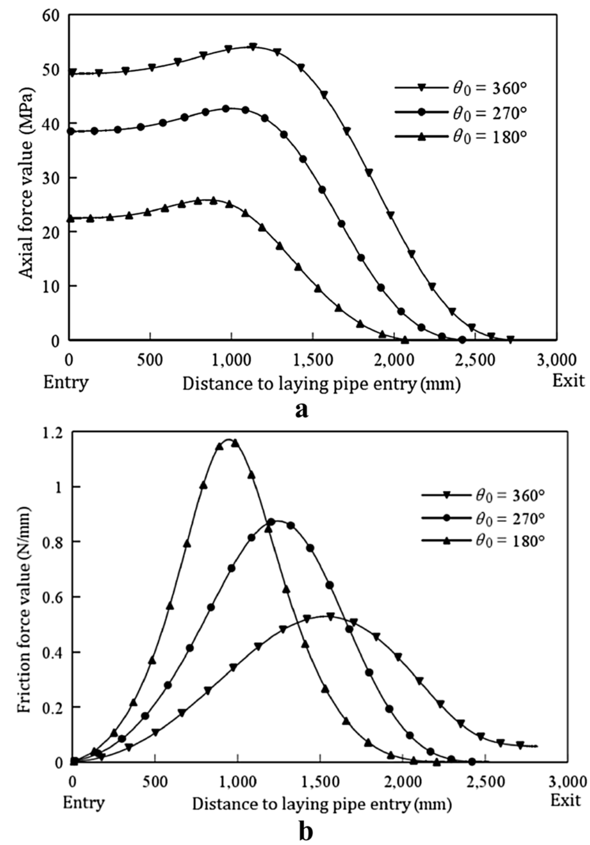

Figure 21 Numerical results with different θ_0: **a** Axial force in the design laying pipe; **b** Friction force in the design laying pipe

Figure 22 shows the wire rod axial force and friction force performance with wire rod diameters of 6.5 mm and 10 mm respectively. When the production of wire rod diameter is 10 mm, the feed speed v_f changes to 68 m/s according to the production process flow. The rotation speed ω_0 for laying pipe is also changed to keep the relationship in Eq. (1). It is indicated from Figure 22(a) and (b) that the axial force and friction force for wire rod 6.5 mm are enhanced than wire rod 10 mm. Thus, it is confirmed that with the higher feed speed and rotation speed, the laying pipe for wire rod ϕ6.5 mm is easier to be worn off than ϕ10 mm.

It is indicated from the numerical results from Figure 19 to Figure 22 that the requirement for higher speed laying pipe curve design should increase the laying pipe axial dimension Z_0 and choose a suitable pipe curve rotated angle θ_0 between 350° and 400°.

6 Conclusions

The paper focused on the laying pipe of laying head device in the hot-rolled high speed wire rod production line. The kinematics and dynamics modeling are first proposed and investigated in this paper with the aim to obtain the wire rod performance while passing through the laying pipe. The statics study and calculation for the wire rod in the laying pipe are carried out by using sectional divided method. A laying pipe curve equation is formulated by considering its design boundary conditions. Thus, numerical results of wire rod velocity and forces can be calculated by the obtained laying pipe equations. With the proposed modeling, kinematics and dynamics results comparison between the designed laying pipe curve and two existing laying pipes are carried out. Some variable parameters of laying pipe curve are calculated with different value, and the results are

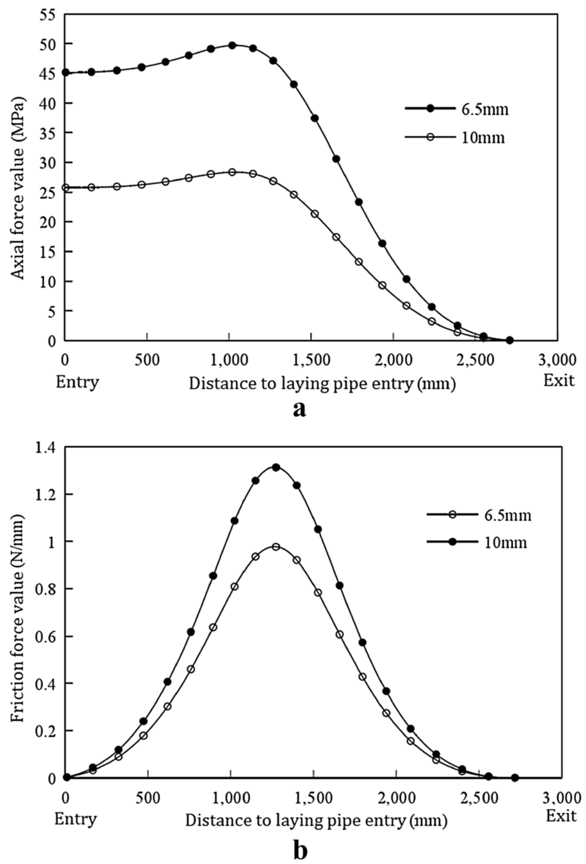

Figure 22 Numerical results with different wire rod dimension: **a** axial force in the design laying pipe; **b** friction force in the design laying pipe

discussed to find suitable design pipe curve parameters for different working conditions. The results of calculation and discussion indicate the proposed method of laying pipe curve design and the research for kinematics and dynamics are feasible for laying pipe application.

Authors' Contributions

SY conceived and studied the laying pipe design method and the force computations. MC contributed the force analysis of the laying pipes. Bin Ma performed the experiments for laying pipe curves. SY and MC wrote the paper. MC, GC and BM reviewed and edited the manuscript. All authors read and approved the final manuscript.

Author Details

[1] College of Material Science and Engineering, Yanshan University, Qinhuangdao 066004, China. [2] University of Cassino and South Latium, Cassino 03043, Italy. [3] HBIS Group Co., Ltd, Handan 056001, China.

Authors' Information

Shuangji Yao, born in 1981, he is currently an associate professor at *Yanshan University*, China. He received his PhD degree from *Beihang University, China*, in 2010. He has joined the study program at LARM during 2007–2008 in Italy. His research interests include the theory of mechanisms, robots, and mechanical research in rolling machine. He is a member of IEEE and ASME.

Marco Ceccarelli, born in 1958, received his Ph.D. degree in Applied Mechanics in 1988. He is a Full-Time Professor of Mechanics of Machinery and Director of LARM, Laboratory of Robotics and Mechatronics at *University of Cassino and South Latium, Italy*. He is a Member of Robotics Commission of IFToMM (The International Federation for the Promotion of Machine and Mechanism Science). He is the IFToMM President. He has written the books "Fundamentals of Mechanics of Robotic Manipulation" in 2004 and "Mecanismos" in 2008 and 2014. His research interests are in mechanics of mechanisms and robots. He is the author/co-author of more than 700 papers, presented at conferences or published in journals, and he has edited 23 books as for conference proceedings and specific topics.

Giuseppe Carbone, born in 1972, is currently an associate professor at *University of Cassino and South Latium, Italy*. He received his PhD degree from *University of Cassino and South Latium, Italy*. He has carried out several periods of research abroad, such as in Germany, Japan, Spain, and China. His research interests include stiffness of multibody robotic systems, robotic hands and grippers, mechatronic designs, design of experimental test-beds. He has published more than 250 peer reviewed papers on the above-mentioned topics.

Bin Ma, born in 1981, is currently a mechanical engineer at *HBIS Group Co., Ltd, China*. He received his master degree on mechatronidcs from *Beijing Institute of Technology, China*, in 2006.

Acknowledgements

We would especially like to thank Dingxuan Zhao, Wantang Fu and Qingtian Zhou for the fruitful discussions, leading to very interesting formulations of problems and deeper insight. Furthermore but not least, we would like to thank Zhifeng Pang, Yongqian Zhao and Renquan Wang for their great help and kindness.

Competing interests

The authors declare that they have no competing interests.

Funding

Supported by China Postdoctoral Science Foundation Project (Grant No. 2017M611184).

Received: 17 January 2019 Accepted: 18 March 2019
Published online: 01 April 2019

References

[1] G Mukhopadhyay, S Bhattacharyya. Wear of laying head pipes in a wirerod mill. *Journal of Failure Analysis and Prevention*, 2013, 13(4): 474-482.

[2] J P Yun, D C Choi, Y J Jeon, et al. Defect inspection system for steel wire rods produced by hot rolling process. *International Journal of Advanced Manufacturing Technology*, 2014, 70(9-12): 1625-1634.

[3] K F Karhausen, H Pawelski. Mechanics and friction in metal rolling. In: *Encyclopedia of Lubricants and Lubrication*. Springer Berlin Heidelberg, 2014.

[4] M Schmidtchen, P Adamyanets, R Kawalla. Model approaches for simulation of processes in rod and wire production. *Materials Science Forum*, 2017, 892: 34-43.

[5] O N Tulupov, A B Moller, S Y Sarancha. Increasing of long products rolling efficiency: modernization of Stelmor air cooling line to obtain sorbitized wire rod. *Solid State Phenomena*, 2017, 265: 1116-1122.

[6] C Liu, Y L Liu, L Y Ma, et al. Finite element analysis of contact between laying head pipe and high-speed wire rod. *Advanced Materials Research*, 2013, 690-693: 3316-3320.

[7] C J Cameim Filho, M B Mansur, P J Modenesi, et al. The effect of hydrogen release at room temperature on the ductility of steel wire rods for pre-stressed concrete. *Materials Science and Engineering A*, 2010, 527: 4947-4952.

[8] S I Platov, V A Nekit, N N Ogarkov. Determination of frictional forces during wire rod drawing process by reverse method. *Solid State Phenomena*, 2017, 265: 1152-1156.

[9] A K Singh. Ergonomic study and design of the pulpit of a wire rod mill at an integrated steel plant. *Journal of Industrial Engineering*, 2015, 2015: 1-11.

[10] Stolarski T A, Tobe S, Stolarski T A, et al. 10. Rolling in metal forming. In: *Rolling Contacts*. John Wiley & Sons, Ltd, 2014.
[11] D Kilcoyne, J Zhang, D Abdelmaseh, et al. Manufacturing laying head pipe path below transformation temperature: WO,2013048818. 2013-04-04 [2019-03-15]. http://www.wanfangdata.com.cn/details/detail.do?_type=patent&id=WO2012US55893.
[12] I S Platov, V A Nekit, N N Ogarkov. Improving the controlled cooling after wire rod rolling in the finishing block of stands. *Materials Science Forum*, 2016, 870: 620-624.
[13] K Fiorucci. Rolling mill coil-forming laying head with path or pipe having dissimilar materials composite construction: US, 2013048821. 2013-04-04 [2019-03-15]. http://www.wanfangdata.com.cn/details/detail.do?_type=patent&id=WO2012US55902.
[14] K Fiorucci. Rolling mill coil-forming laying head with path or pipe components formed by laser sintering process: US, 2013075515. 2013-03-28 [2019-03-15]. http://www.wanfangdata. com.cn/details/detail.do?_type=patent&id=US201213611142.
[15] K Fiorucci. Rolling mill laying head pipe having modular construction: WO, 2013048774. 2013-04-04 [2019-03-15] http://www.wanfangdata.com.cn/details/detail.do?_type=patent&id=WO2012US55322.
[16] Siemens Industry in Regenerative. Regenerative laying pipe and method of changing the interior surface of a laying pipe: EP, 2613897. 2013-07-17[2019-03-15] http://www.wanfangdata.com. cn/details/detail.do?_type=patent&id=EP20110755528.
[17] A A Zlobin, S A Zlobin. Technology and equipment of a space-saving metallurgical complex for producing wire rod in coils. *Metallurgist*, 2013, 57(1-2): 57-63.
[18] H M Liu, S J Yao, L P Yang, et al. Research and improvement of the pipe space curve of high-speed laying head. *Engineering Science*, 2006, 8(11): 80-85.
[19] J Liu, Q Zhou. Design of the pipe of laying head and its load analysis. *Iron & Steel*, 1997, 32(5): 75-80. (in Chinese)
[20] A S Karandaev, I A Yakimov, O I Petukhova, et al. Power parameters of electric drives of five-stand wire rod mill with four-roll passes. *2017 IEEE Conference of Russian Young Researchers in Electrical and Electronic Engineering (EIConRus)*, 2017: 1524-1528.
[21] J Tominaga, K Y Wakimoto, T Mori, et al. Manufacture of wire rods with good descaling property. *Transactions of the Iron & Steel Institute of Japan*, 2006, 22(8): 646-656.
[22] D W Wang, W Wang. Analysis and handling of laying head dynamic balancing fault at high speed wire rod mill. *Tianjin Metallurgy*, 2015, 4: 75-78. (in Chinese)
[23] F Mulinaris, G Verlini, G Salvador. Danieli high-speed wire rod mills: advanced technology and high-level performances. *Iron & Steel*, 2006, 41(6): 83-86.
[24] G W Xiao. Analysis on laying head fault at high speed wire rod rolling and controlling measures. *Tianjin Metallurgy*, 2015, 6: 49-55. (in Chinese)
[25] A Konyukhov, K Schweizerhof. On some aspects for contact with rigid surfaces: Surface-to-rigid surface and curves-to-rigid surface algorithms. *Computer Methods in Applied Mechanics and Engineering*, 2015, 283: 74-105.
[26] L I Longjian, G Liu. Flow friction analysis of the water-cooled nozzle in the high-speed wire rod rolling process. *Journal of Chongqing University*, 2014, 37(4): 88-92.
[27] S V Rodinkov, V V Pavlenko, V G Drozd, et al. Tendencies of development of stand construction in rolling mills. *Agricultural & Biological Chemistry*, 2015, 51(3): 883-890.
[28] S J Yao. *Research on high-speed wire pipe of laying head and working quality improvement*. Qinhuangdao: Yanshan University, 2006. (in Chinese)
[29] F Yu, Y Hao. Application of mathematical modeling in two-stage rolling of hot rolled wire rods. *Journal of Materials Processing Tech.*, 2014, 214(9): 1962-1970.